

# Calculation of shapes of dipolar domains in two-dimensional films: Effect of dipole tilt

M. A. Mayer and T. K. Vanderlick<sup>a)</sup>

Department of Chemical Engineering, University of Pennsylvania, Philadelphia, Pennsylvania 19104-6393

(Received 23 June 1995; accepted 6 September 1995)

Dispersed domains in two-dimensional two-phase systems often exhibit complex and intriguing morphologies. For many of these systems, it is possible to predict the shape of such a domain through an evaluation of the free energy. In this paper, we extend our previous numerical technique for calculating domain shapes by allowing for tilted dipoles; the original technique assumed dipole moments oriented normal to the system plane. The solution diagram is presented in the vicinity of the primary shape transition for varying tilt angles. We find that circular domains are only stable in the absence of dipole tilt. Moreover, we find that the discontinuous transition found when the dipoles are vertical gives way to continuous elongation with increasing dipole tilt. Interestingly, it appears that the critical angle is independent of domain size. © 1995 American Institute of Physics.

## I. INTRODUCTION

In recent years, much work has been undertaken in the study of quasi two-dimensional systems which display phase separation. Drawing much of the attention are those systems which display interesting morphologies, either through shapes of individual domains or through patterns formed by the arrangement of domains. These include ferromagnetic fluids confined between parallel plates,<sup>1-3</sup> thin magnetic films,<sup>4</sup> superconductors,<sup>5,6</sup> and insoluble monolayers at air/water interfaces.<sup>7-9</sup> While each of these systems is independently unique, they share the common property of being composed of a continuous field of parallel-oriented dipoles—electrostatic or magnetostatic. Consequently, when they separate into two phases, they display similar morphologies.

Of particular interest to the authors of this paper are those studies which attempt to predict the shapes of isolated domains (especially in the context of insoluble monolayers). While many experimentally observed domain shapes clearly result from growth kinetics,<sup>10</sup> it has also been observed that domain shape can be reproducibly controlled by manipulating physical conditions such as area or temperature.<sup>7</sup> This latter observation strongly suggests that the shape of a domain is, in fact, a function of the state of the system and thus predictable through an energy minimization analysis. Historically, such analyses have followed one of three approaches:

- (1) Direct comparison of the energies of two or more given domain shapes.<sup>11-14</sup>
- (2) Evaluation of the stability of a given domain shape.<sup>15,16</sup>
- (3) Dynamic evolution of domain shape as driven by an energy gradient.<sup>1,17</sup>

One powerful technique notably absent from this list of approaches is direct solution of the first functional derivative of energy.<sup>18</sup> In particular, if one knows explicitly the functional relationship between the shape of a domain and the energy of that domain, it is theoretically possible to solve directly for shapes corresponding to energy extrema. These

shapes (which shall henceforth be referred to as stationary shapes) satisfy the so-called Euler–Lagrange equation, formed by setting the first functional derivative of energy with respect to the shape function equal to zero. The stability of these stationary shapes can be subsequently established by examining the second functional derivatives, thereby distinguishing energy minima from energy maxima and saddle points. While it is true that dynamic evolution of domain shape as driven by the energy gradient also ultimately solves the Euler–Lagrange equation, it does so rather inefficiently; furthermore, it will only find stable solutions. This approach to domain shapes analysis is best left to examining the pathways and kinetics of shape evolution.

In the prediction of domain shapes, as with many other problems, the Euler–Lagrange equation cannot be solved analytically. If a solution is to be found, it must be done so numerically. For this the method of finite elements<sup>19</sup> is particularly well suited. Approximating the shape with finite element functions and forming Galerkin weighted residuals, the original variational problem reduces from an integral–differential equation to a set of nonlinear algebraic equations which can be readily solved by an iterative technique such as Newton’s method. Such numerical solution of the Euler–Lagrange equation is a standard in engineering mathematics and has been used successfully in many similar applications, e.g., the prediction of the shape of a rotating liquid drop.<sup>20</sup>

We have recently demonstrated<sup>21</sup> that the calculus of the variations approach can indeed be used to solve for the shape of an isolated domain; our study was done in the context of insoluble monolayers and was based on the free-energy functional proposed by McConnell *et al.*<sup>11</sup> This functional identifies two-shape dependent contributions to a domain’s energy: interfacial tension and repulsion between dipoles. As we quickly discovered, the challenges in applying the variational approach to this particular problem—the reasons it was probably not done earlier—are purely in the evaluation of the derivatives of the energy functional. This approach, however, has two major advantages over the three used in prior calculations which make the extra effort extremely worthwhile. First and foremost, the solution does not come from a predetermined list of domain shapes (or shape

<sup>a)</sup>To whom correspondence should be addressed.

classes). We therefore need not worry about whether the true energy minimizing shape has even been considered. Given sufficient numerical discretization (and an accurate energy model), all computed stable solutions will minimize the domain's energy, at least locally. Second, nonstable stationary shapes are found along with stable stationary shapes. Solution branches can therefore be tracked through turning points and new branches located at bifurcations, allowing the parameter space to be systematically charted.

The results presented in our paper, which introduced the variational approach to domain shape calculations, were based on an energy functional which assumed vertical dipoles, i.e., no component of the dipole moment parallel to the plane of the domain. This previous study shall be referred to as the vertical case. Five key results were found in this vertical case. Circles are always stationary shapes, although not always energy minima. All other stationary shapes can be categorized as bilobes, trilobes, 4-lobes, etc. Each of these solution branches bifurcates from the branch of circular solutions, and does so subcritically. The only domain shapes which represent energy minima are circles (when interfacial tension dominates) and bilobes (when dipolar repulsion dominates). Because these branches bifurcate subcritically, the transition from circular domains to bilobed domains is discontinuous.

In this study, we extend our previous results by relaxing the constraint that the dipoles are normal to the system plane. Indeed, it is not difficult to recognize the physical sources of dipole tilt, e.g., the orientation of the polar head group in an insoluble monolayer or the direction of the magnetic field enclosing a ferromagnetic fluid. Because of this very real possibility of dipole tilt, any thorough study of domain shape should consider its possible effect. We should note that while most domain shape calculations in the literature assume vertical dipoles, this is not the first study to allow for tilted dipoles; McConnell *et al.*<sup>12</sup> reported the effect of dipole tilt on the transition from circular to elliptical domains. However, this is, to the best of our knowledge, the first study to use the variational approach to compute domain shapes and to account for dipole tilt. In this paper, we will briefly review the energy model and solution algorithm, present our results, compare these results where applicable to those of McConnell *et al.*, and discuss relevance to physical systems.

## II. METHOD

To fully appreciate the domain shapes predicted in this study, the reader needs to be familiar with two key background elements: the energy model and the solution algorithm. Because this is an extension to the vertical dipole study, most of this information has already been published in some detail;<sup>21</sup> the incorporation of tilted dipoles requires but minor adaptation. For this reason, only an abbreviated overview of the energy model and solution algorithm is provided here.

Following the analysis of McConnell *et al.*,<sup>11</sup> two-shape dependent contributions to the energy of the domain are identified. Line tension, arising from the excess free energy associated with the interface between the domain and its surroundings, acts to minimize perimeter—promoting compact

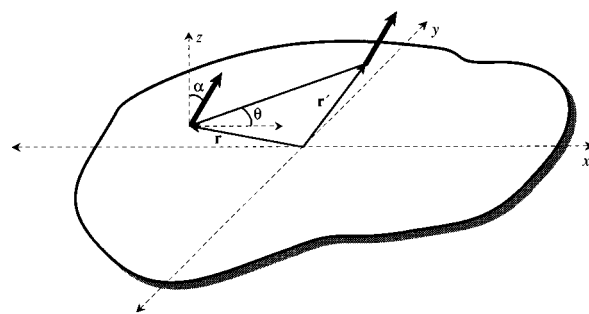


FIG. 1. Coordinate system used to define  $\alpha$  and  $\theta$  of Eq. (2.2). The origin is located at the center of mass of the domain with the  $x$  and  $y$ -axes in the plane of the domain and the  $x$  axis aligned with the direction of dipole tilt. The angle between dipole moment and the  $z$  axis is represented by  $\alpha$ . The angle between  $\mathbf{r}-\mathbf{r}'$  and the  $x$  axis is represented by  $\theta$ .

domains. Countering this, electrostatic repulsion acts to increase the average distance between individual dipoles—promoting elongated domains. Combined, these two opposing contributions create the overall energy potential

$$F = \lambda P + \frac{\mu^2}{2} \int_D \int_D \int_D \int_D \frac{g(|\mathbf{r}-\mathbf{r}'|)}{|\mathbf{r}-\mathbf{r}'|^3} \Psi(\mathbf{r}, \mathbf{r}') d^2 \mathbf{r}' d^2 \mathbf{r}, \quad (2.1)$$

where  $\Psi$ , which shall be referred to as the tilt factor, is defined as

$$\Psi(\mathbf{r}, \mathbf{r}') = 1 - 3 \sin^2 \alpha \cos^2 [\theta(\mathbf{r}, \mathbf{r}')]. \quad (2.2)$$

Here  $\lambda$  and  $P$  represent, respectively, the line tension and the domain perimeter. The parameter  $\mu$  represents the excess dipole density of the domain relative to the surrounding phase. The integration limit  $D$  represents all points in the domain and  $g(r)$  the pair distribution of dipoles. The angles  $\alpha$  and  $\theta$  are related to the orientation of the dipole moment. Their exact definitions are most easily conveyed, as illustrated in Fig. 1, by defining the  $x$ - $y$  plane such that it is coplanar with the domain, its origin is located at the center of mass of the domain, and the  $x$  axis aligns with the direction of dipole tilt. In this context,  $\alpha$  is the angle between the dipole moment and the  $z$  axis and  $\theta$  is the angle between  $\mathbf{r}-\mathbf{r}'$  and the  $x$  axis. The only difference between (2.1) and the energy functional of the vertical dipole study<sup>21</sup> is the tilt factor,  $\Psi$ , found in the integrand of the electrostatic term.

As in our vertical dipole calculation, we use the Heaviside function as the basis for the dipole distribution function,  $g(r)$ , i.e., its value is 0 when  $r < \delta$  and 1 when  $r > \delta$ . The basic physical requirements of  $g(r)$  are that it vanish at small separations, to avoid overlap of dipoles, and that it approach unity at large separations, as dipole distribution becomes uncorrelated. The Heaviside function is the simplest expression which meets these criteria. Other domain shape calculations have used (either implicitly or explicitly) an alternate pair distribution function proposed by McConnell<sup>15</sup>

$$\tilde{g}(r) = \frac{r^3}{\sqrt{r^2 + \Delta^2}^3}. \quad (2.3)$$

The primary advantage of this alternate expression is that it allows the double area integral of (2.1) to be reduced analytically to a double contour integral. Solution of the Euler–Lagrange equation, however, never requires evaluation of the domain energy, only its first and second derivatives. Because the solution algorithm which follows produces double contour expressions for these derivatives, use of this alternate  $g(r)$  yields us no particular advantage.

The numerical algorithm used to predict domain shapes by solution of the Euler–Lagrange equation is essentially a five-step process; outlined below. As with the variational approach itself, none of these steps is inherently novel or complicated. The sole complication—evaluation of the derivatives of the energy functional—can be overcome by applying the techniques outlined in our vertical dipole paper;<sup>21</sup> the inclusion of the tilt factor again requires only trivial adaptation.

(1) The problem parameters and variables are identified though dedimensionalization and discretization. Scaling all lengths by  $\delta$  and all energy terms by  $\lambda\delta$  yields three parameters: the tilt angle,  $\alpha$ ; the ratio of dipole strength to line tension,  $\Gamma$  ( $=\mu^2/\lambda$ ); and the domain area,  $A_0$ . Approximating the shape function as a linear combination of  $N$  cubic finite element functions yields  $2N$  variables—two coefficients per finite element node.

(2) The problem constraints are introduced into the energy functional through the method of Lagrange multipliers. Specifically, the area of the domain is held at  $A_0$  and the center of mass fixed at the origin. The latter constraint is purely mathematical—eliminating translational degeneracy—and no physical interpretations should be inferred from it. Introduction of these two constraints produces three additional variables, one Lagrange multiplier for area and two for center of mass.

(3) The governing equations— $2N$  derivatives of  $F$  with respect to the finite element coefficients and three side constraints—are solved iteratively using Newton's method.

(4) The stability of the solution is evaluated to determine if it is, in fact, an energy minimum. Specifically, using a technique introduced by Golub,<sup>22</sup> the extreme values of the second variation of  $F$  are found such that only those shapes which preserve area and produce no domain translation are considered as valid perturbations.

(5) Finally, the solution is mapped over parameter space by stepping through  $\Gamma$ ,  $\alpha$ , or  $A_0$  using zero<sup>th</sup> order continuation. With the solution just computed for one set of parameter values as an initial guess, steps 3 and 4 are repeated to compute the solution for a new set of parameter values (ideally not too different from the original set).

Although this solution algorithm is nearly identical to that used for the vertical dipole calculation, a few minor revisions are necessary to accommodate the inclusion of the tilt factor. Because these were not addressed when we first introduced the algorithm for the vertical case, they are mentioned here for completeness. In the vertical case, rotation of

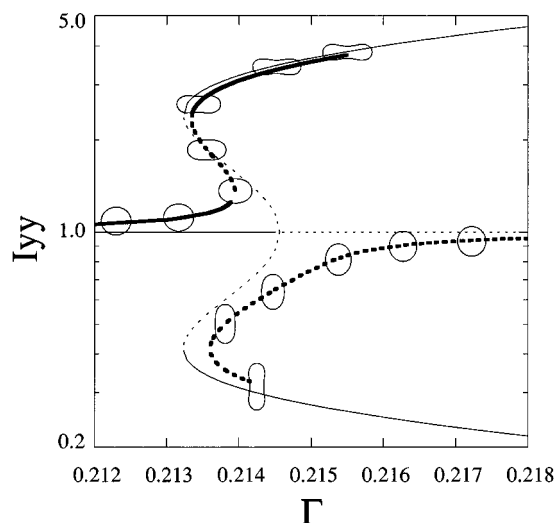


FIG. 2. Solution diagram of domain shape both with and without dipole tilt. The  $I_{yy}$  moment of inertia (normalized to circular domains) is plotted as a function of dimensionless dipole strength. Values of  $I_{yy}$  greater than 1 indicate elongation along the  $x$  axis (tilt direction). Values less than 1 indicate elongation along the  $y$  axis. Domain area is  $2500\pi\delta^2$ . Stable solutions are shown as solid lines; unstable solutions as broken lines. The solution for tilted dipoles ( $\alpha=1.5^\circ$ ) is shown with heavy lines; the solution for vertical dipoles ( $\alpha=0^\circ$ ) as a light line. Inset figures depict the shape of the domain at various points along the solution curve.

the domain has no effect on the value of the energy functional. The presence of  $\Psi(\mathbf{r},\mathbf{r}')$  breaks this rotational degeneracy. The vertical dipole algorithm requires a constraint to prevent rotation. This constraint is not only unnecessary in the tilted dipole algorithm, including it would be inappropriate; the energy functional should dictate domain orientation, not the solution algorithm. The remaining (minor) revisions handle differentiation of the energy functional, in particular the electrostatic term, in light of the tilt factor. For the first functional derivatives, the only change necessary is the inclusion of the tilt factor in the integrand. The sole dependency of the electrostatic integral on shape comes through its limits of integration. Thus differentiation (by Liebnitz rule) simply involves evaluating the integrand at the limits. For the second functional derivatives, however, two changes are necessary. Again, the tilt factor must be added to the electrostatic terms that were found in the vertical case. In addition, application of chain rule produces an extra term due to the differentiation of the tilt factor, which does depend on shape in the first derivative.

### III. RESULTS AND DISCUSSION

We begin discussion of our results by comparing the solution diagram for tilted dipoles ( $\alpha=1.5^\circ$ ) to that for vertical dipoles ( $\alpha=0^\circ$ ). Specifically, we focus on the region near the bifurcation from circular to bilobed domains found in the vertical case, as depicted in Fig. 2. Stationary domain shape, as measured by the  $I_{yy}$  moment of inertia normalized to a circular domain, is examined as a function of dimension-

less dipole strength,  $\Gamma$ . Because moment of inertia alone cannot fully describe shape, representative shapes calculated for the tilted dipole case are superimposed on the appropriate solution curve. The termination of the bilobed branches is not a mathematical endpoint of these curves. Rather, as previously discussed,<sup>21</sup> it is the limit of computability. Due to a rapidly decaying energy gradient, continuation beyond this point faces severely diminishing returns.

Comparing the two cases shown in Fig. 2, it is immediately apparent that dipole tilt has a profound effect on the solution diagram. The vertical dipole solution exhibits a branch representing circular domains from which a branch representing bilobed domains bifurcates. The inclusion of dipole tilt breaks<sup>23</sup> this bifurcation. The tilted dipole solution also exhibits two branches. They are, however, no longer connected and have undergone a reorganization. Each of these branches contains a regime that evolved from the circular branch in the vertical calculation and a regime that evolved from the bilobed branch. Both branches now represent bilobed domains. One represents domains elongated parallel to the direction of dipole tilt. The other represents domains elongated perpendicular to tilt. Loss of solution bifurcations with the introduction of a symmetry breaking conditions is a fairly common occurrence and is by no means unique to domain shapes. The classic example is the bending of a rigid rod due to compression.<sup>23</sup> Given a rod which is initially straight, the direction it bends (at critical load) will occur with equal probability. Given a rod which is initially kinked, it will bend preferentially in the direction of the kink, and will do so at a smaller critical load.

This breaking of the bifurcation and reorganization of the solution branches has two significant consequences. First, circular domains are no longer solutions to the Euler–Lagrange equation—except in the trivial case when  $\Gamma=0$ . The circular domains found in the vertical case have evolved into nearly circular ovoid domains (geometrically, they are not elliptical). For small  $\Gamma$ , these ovals elongate parallel to the direction of dipole tilt and are stable solutions. For large  $\Gamma$ , they elongate perpendicular to tilt and are unstable (just as circles are unstable for large  $\Gamma$  in the vertical case). Second, the only domain shapes ever to be stable are those which elongate parallel to tilt.

Both of these results are easily explainable based solely on the definition of  $\Psi$  in Eq. (2.2). Clearly the value of  $\Psi(\mathbf{r},\mathbf{r}')$  is greater when  $\mathbf{r}-\mathbf{r}'$  lies perpendicular to the  $x$  axis (the direction of dipole tilt) than when it lies parallel. This immediately explains why only those solutions representing elongation parallel to dipole tilt are stable. It also explains why circular domains are not solutions. Specifically, the first functional derivative of the electrostatic contribution to Eq. (2.1) is nonzero for circular domains—an infinitesimal elongation along the  $x$  axis reduces the energy while an infinitesimal compression (negative elongation) increases the energy. As circular domains minimize domain perimeter, the first functional derivative of the interfacial contribution to Eq. (2.1) must be zero for circular domains. Because these are the only two contributions to Eq. (2.1), the first functional derivative of the domain energy must be nonzero for

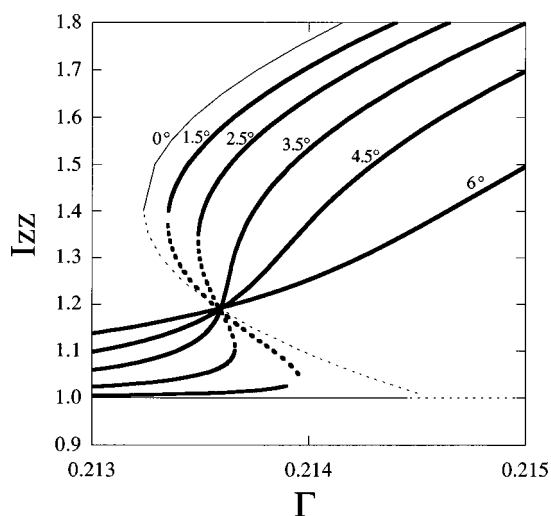


FIG. 3. Solution branches for domains elongated parallel to dipole tilt for six different tilt angles: 0°, 1.5°, 2.5°, 3.5°, 4.5°, and 6°. The  $I_{zz}$  moment of inertia is plotted vs dimensionless dipole strength. When  $I_{zz}=1$  the domain is circular. All noncircular domains have an  $I_{zz}$  value greater than 1. Domain area is  $2500\pi\delta^2$ . Solid lines represent stable solutions; broken lines represent unstable solutions.

circular domains. Thus they are not solutions to the Euler–Lagrange equation.

Although not necessarily as interesting as the differences, the tilted dipole solution diagram also has many similarities to the vertical case. The only stable (noncircular) solutions are bilobes. The solution diagram exhibits additional branches representing trilobes, 4-lobes, etc. These branches bifurcate from the regime which evolved from the circular branch; they do so at the same values of  $\Gamma$ . Because so little about these solutions has changed and because they do not represent stable domain shapes, they are not included in Fig. 2.

Having examined the effects that the inclusion of dipole tilt has on the solution diagram, we proceed by examining the effect degree of tilt has on the solution. Focusing on the branch of domains elongated parallel to the direction of dipole tilt, Fig. 3 replots the solution diagram for multiple tilt angles. The  $I_{zz}$  moment of inertia is now used as the measure of shape rather than  $I_{yy}$  as it provides more accurate information about degree of elongation. The  $I_{yy}$  moment was used in Fig. 2 because  $I_{zz}$  provides no information about direction of elongation. Just as it was immediately apparent that including dipole tilt had a profound effect on the connectivity of solution branches, it is equally apparent that changing the angle of dipole tilt affects the fundamental character (shape) of the branch supporting stable solutions and, thus, the nature of the transition from compact to elongated domains.

For small tilt angles, the solution branch passes through a pair of turning points in  $\Gamma$ —remnant of the subcritical bifurcation from the vertical case. Between these turning points, the solution shapes are unstable. Everywhere else along the branch, they are stable. Hence, exactly two stable solutions exist for all values of  $\Gamma$  between the turning points—one from the regime of compact domains and one

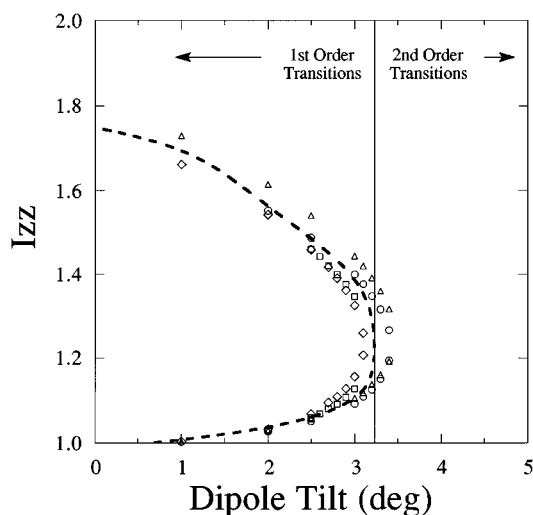


FIG. 4. Shape-transition diagram. Below the critical tilt ( $\approx 3.3^\circ$ ), the two values associated with the discontinuous transition are plotted as a function of tilt angle. Above the critical tilt, domains elongate continuously. Results are shown for four domain areas:  $2500\pi\delta^2$  ( $\circ$ ),  $10,000\pi\delta^2$  ( $\square$ ),  $40,000\pi\delta^2$  ( $\diamond$ ), and  $250,000\pi\delta^2$  ( $\triangle$ ). The broken line through the data and the vertical line dividing discontinuous transitions from continuous elongation are visual guides.

from the regime of elongated domains. Because these two solutions never intersect, the transition from compact to elongated domains must be discontinuous, i.e., first order, just as was found in our vertical dipole calculation. For large tilt angles, however, the solution branch does not go through any such turning points and all solutions found on it are stable. The transition from the compact to the elongated regime is, in this case, continuous. The angle at which the changeover from discontinuous transition to continuous elongation occurs shall be referred to as the critical tilt angle. For very large tilt, the elongation of the domain occurs too gradually to be considered a transition at all.

To better envision the changeover from discontinuous to continuous elongation, it is convenient to create a shape-transition diagram, as shown in Fig. 4. Below the critical tilt angle, the  $I_{zz}$  values of the compact and elongated solutions associated with the discontinuous shape transition are plotted as a function of tilt angle. For this purpose, the transition is defined to occur at that  $\Gamma$  for which the free energy of the compact and elongated domains is equal, i.e., when the global minimum switches branches. Interestingly, as suggested by the shape-transition diagram shown in Fig. 4, the critical angle appears to be independent of domain size with a value of approximately  $3.3^\circ$ . Despite the apparent similarity to thermodynamic phase diagrams, the reader is cautioned against carrying this analogy too far—lever rule, for example, does not apply.

Finally, as moment of inertia (or any other scalar) cannot alone fully describe domain shape, comparisons of solution diagrams based on moment of inertia cannot fully describe the relationship between tilt angle and domain shape. A table of representative solution shapes is therefore depicted in Fig. 5 for various degrees of dipole tilt angle and domain elonga-

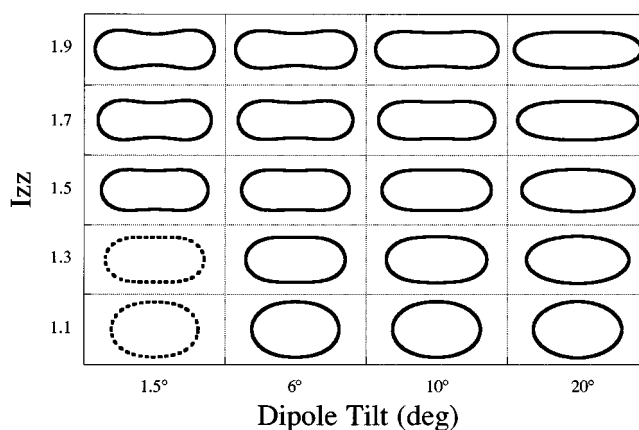


FIG. 5. Domain shapes calculated for four tilt angles ( $1.5^\circ$ ,  $6^\circ$ ,  $10^\circ$ , and  $20^\circ$ ) and five values of  $I_{zz}$  (1.1, 1.3, 1.5, 1.7, and 1.9). Domain area of all shapes is  $2500\pi\delta^2$ . The two domains shown with broken perimeters are unstable solutions.

tion. Clearly, for any given value of  $I_{zz}$  the concavity of domain shape decreases with increasing tilt. The dogbone shapes found for small  $\alpha$  give way to cigarlike shapes as  $\alpha$  increases.

As mentioned in the introduction, this is not the first study to consider dipole tilt in the calculation of domain shapes. McConnell *et al.*<sup>12</sup> reported the effects of dipole tilt on the transition from circular to elliptical domains. Our results agree with theirs on three points. Both predict that circles are solutions only in the absence of dipole tilt. Both predict that domain elongation occurs in the direction of dipole tilt. Both predict the eventual loss of a clear-shape transition with large tilt angle. Their results, however, fail to predict discontinuous shape transitions, even for vertical dipoles. They obviously therefore could not address the question of a critical tilt angle, much less its relationship to domain size. Moreover, because the only shapes they considered were ellipses, the fact that domain shape changes with tilt at fixed elongation could not be observed.

The usefulness of any theoretical calculation is, of course, its ability to provide insight—either quantitative or qualitative—into the physical system it is designed to model. Quantitative comparison of the shapes predicted in this calculation with those observed experimentally requires the ability to measure (or control) the physical parameters  $\delta$ ,  $\lambda$ ,  $\mu$ , and  $\alpha$ . Unfortunately, measurement of the dipole cutoff parameter ( $\delta$ ) is not realistically possible; real pair distributions are not simple step functions. Although its magnitude must be on the scale of the distance between nearest neighbor dipoles, its exact value will most likely remain an adjustable parameter. The feasibility of measuring the remaining three parameters varies with the experimental system. For ferromagnetic fluids, line tension ( $\lambda$ ) can be easily measured experimentally<sup>24</sup> and dipole density ( $\mu$ ) and tilt angle ( $\alpha$ ) are directly controlled through the applied magnetic field.<sup>1-3</sup> Nonetheless, we could find no reference to ferrofluid shape studies utilizing tilted magnetic fields. For insoluble monolayers, measurement of these three parameters is not so straightforward. For domains composed of vertical dipoles,

various methods have been devised to back out the values of  $\mu$  and  $\lambda$  from shape measurements;<sup>17,25</sup> these do not, however, consider tilted dipoles. Moreover, for monolayers composed of tilted dipoles, measurement of the tilt angle is frustrated by many obstacles. Both the location and orientation of the functional group generating the dipole (e.g., the phosphorous–nitrogen pair in phospholipids) must be known as well as the profile of the electrostatic permeativity through the water interface.<sup>20,26–30</sup> Assumably due to these obstacles, we could find no reference to quantitative measurement of tilt angle in phase separating insoluble monolayers. As it is not the intention of this paper to introduce experimental methods or techniques, this void will not be filled here. Note that while techniques do exist for measuring the tilt angle of hydrocarbon tail groups, e.g., Brewster angle microscopy,<sup>31</sup> the dipole moment is associated primarily with the head group,<sup>27</sup> not the tail. We are not familiar enough with the other systems listed in the introduction to speculate on the plausibility of quantitative measurement.

Because quantitative comparisons cannot yet be drawn between our results and experimental observations, the usefulness of this study is currently in its ability to make qualitative predictions. While most of these are immediately apparent from the solution discussed above, the practicality of these results is not necessarily as obvious. Our results predict that circular domains should never be found in the presence of dipole tilt. The degree of elongation is, however, extremely small for most values of  $\Gamma$  below the transition. Therefore, except in the region of the elongation transition, experimental detection of noncircularity would require extremely sensitive image analysis equipment. Our results predict that domain elongation should parallel dipole tilt. The ability to observe this experimentally will depend on the ability to find the direction of the dipole tilt. In the case of ferrofluids this should be trivial—it is the same as the magnetic field. In the case of insoluble monolayers, however, each domain may have a unique tilt direction. (This assumes, of course, that each domain has a single tilt direction;<sup>32</sup> if the domain has more than one, then this study is not applicable to that system.) Assuming that tilt direction can be measured at all, it would have to be measured *in situ* for each domain whose shape is being observed. Finally, our results predict a critical tilt angle of only 3.3°. This is quite small by most practical standards. If a domain is not composed of vertical dipoles,<sup>33</sup> it is highly probable that the tilt will be greater than the critical value. It should be expected therefore that not all monolayer systems (possibly only a minority) will exhibit the characteristic evidence of discontinuous transitions, e.g., shape coexistence and hysteresis. Stine and Stratmann<sup>34</sup> have, however, observed shape coexistence experimentally in sterylamine monolayers—confirming that discontinuous transitions do exist.

#### IV. CONCLUSIONS

Inclusion of tilted dipoles in the numerical calculation of domain shapes produces a number of significantly different results from the calculation with vertical dipoles. The circular domains predicted in the vertical case give way to nearly circular ovoid domains. The bifurcation between bilobed do-

main and circles found in the vertical case has been broken for tilted dipoles. Domains, rotationally degenerate in the vertical case, prefer to elongate parallel to the direction of dipole tilt. Furthermore, the solution diagram is affected not only by the presence of dipole tilt, but also by the degree of tilt. Small tilt results in discontinuous shape transitions. Large tilt results in continuous elongation. Moreover, tilt angle influences the character of domain shape beyond when and how transitions occur. With increasing tilt, the degree of concavity diminishes; dogboned domains give way to cigars.

Future work in domain shape calculation should continue to expand the energy functional to incorporate more of the aspects of real physical systems. Such aspects should include (but are by no means limited to) anisotropic line tension, inhomogeneity of dipole tilt within a domain, and interdomain interactions. In addition, because physical systems are found at finite temperature, entropic aspects should also be examined. Such studies will most likely involve Monte Carlo simulations of the domain shape.

#### ACKNOWLEDGMENTS

We gratefully acknowledge the support for this work provided by the National Science Foundation through the Presidential Young Investigator Program (Grant No. CTS-89-57051), by the David and Lucile Packard Foundation, and by a grant from NATO (No. CRG 890971). In addition, we wish to express our gratitude for the fellowship awarded to M. A. M. by Procter and Gamble. Finally, we would like to thank Dr. H. Möhwald at the Universität Mainz for all of his continued interest and insight over the last five years.

- <sup>1</sup>S. A. Langer, R. E. Goldstein, and D. P. Jackson, *Phys. Rev. A* **46**, 4894 (1992).
- <sup>2</sup>A. J. Dickstein, S. Erramilli, R. E. Goldstein, D. P. Jackson, and S. A. Langer, *Science* **261**, 1012 (1993).
- <sup>3</sup>R. E. Rosenweig, *Ferrohydrodynamics* (Cambridge University, Cambridge, 1982), Chap. 7.
- <sup>4</sup>T. Garel and S. Doniach, *Phys. Rev. B* **26**, 325 (1982).
- <sup>5</sup>R. P. Huebener, *Magnetic Flux Structures in Superconductors* (Springer, New York, 1979).
- <sup>6</sup>L. D. Landau, *Zh. Eksp. Teor. Fiz.* **7**, 371 (1937).
- <sup>7</sup>M. Flörsheimer and H. Möhwald, *Chem. Phys. Lipids* **49**, 231 (1989).
- <sup>8</sup>V. Tschärner and H. M. McConnell, *Biophys. J.* **36**, 409 (1981).
- <sup>9</sup>C. M. Knobler, *Science*, **249**, 870 (1990).
- <sup>10</sup>A. Müller and H. Möhwald, *J. Chem. Phys.* **86**, 4258 (1987).
- <sup>11</sup>D. J. Keller, J. P. Korb, and H. M. McConnell, *J. Phys. Chem.* **91**, 6417 (1987).
- <sup>12</sup>H. M. McConnell and V. T. Moy, *J. Phys. Chem.* **92**, 4520 (1988).
- <sup>13</sup>T. K. Vanderlick and H. Möhwald, *J. Phys. Chem.* **94**, 886 (1990).
- <sup>14</sup>M. A. Mayer and T. K. Vanderlick, *Langmuir* **8**, 3131 (1992).
- <sup>15</sup>H. M. McConnell, *J. Phys. Chem.* **94**, 4728 (1990).
- <sup>16</sup>J. M. Deutch and F. E. Low, *J. Phys. Chem.* **96**, 7097 (1992).
- <sup>17</sup>R. E. Goldstein and D. P. Jackson, *J. Phys. Chem.* **98**, 9626 (1994).
- <sup>18</sup>I. M. Gelfand and S. V. Fomin, *Calculus of Variations* (Prentice-Hall, Englewood Cliffs, NJ, 1963).
- <sup>19</sup>G. Strang and G. J. Fix, *An Analysis of Finite Element Method* (Prentice-Hall, Englewood Cliffs, NJ, 1973).
- <sup>20</sup>R. A. Brown and L. E. Scriven, *Philos. Trans. R. Soc. London* **297**, 5 (1980).
- <sup>21</sup>M. A. Mayer and T. K. Vanderlick, *J. Chem. Phys.* **100**, 8399 (1994).
- <sup>22</sup>G. H. Golub, *SIAM Rev.* **15**, 318 (1973).
- <sup>23</sup>G. Iooss and D. Joseph, *Elementary Stability and Bifurcation Theory* (Springer, New York, 1990), Chap. 29.
- <sup>24</sup>R. E. Goldstein, Princeton University (private communication).
- <sup>25</sup>D. J. Benvegnu and H. M. McConnell, *J. Phys. Chem.* **96**, 6820 (1992).

- <sup>26</sup>P. Dynarowicz, M. Paluch, and B. Waligora, *J. Colloid Interface Sci.* **124**, 436 (1988).
- <sup>27</sup>Ken Blasie, University of Pennsylvania (private communication).
- <sup>28</sup>V. Vogel and D. Möbius, *J. Colloid Interface Sci.* **126**, 408 (1988).
- <sup>29</sup>O. N. Oliveira, D. M. Taylor, T. J. Lewis, S. Salvagno, and C. J. M. Stirling, *J. Chem. Soc. Faraday Trans. 1* **85**, 1009 (1989).
- <sup>30</sup>D. M. Taylor, O. N. Oliveira, and H. Morgan, *J. Colloid Interface Sci.* **139**, 508 (1990).
- <sup>31</sup>K. Hosoi, T. Ishikawa, A. Tomioka, and K. Miyano, *Jpn. J. Appl. Phys.* **32**, 135 (1993).
- <sup>32</sup>X. Qiu, J. Ruiz-Garcia, K. J. Stine, C. M. Knobler, and J. V. Selinger, *Phys. Rev. Lett.* **67**, 703 (1991).
- <sup>33</sup>In some insoluble monolayer systems, the dipole moment arises from an ionic dissociation, e.g., fatty acids. For these systems, it can probably be assumed that dipole moment is vertical.
- <sup>34</sup>K. J. Stine and D. T. Stratmann, *Langmuir* **8**, 2509 (1992).